Semiconductor Sensors

Frank Hartmann[a]

[a] *Institut für Experimentelle Kernphysik, KIT, Germany*

Abstract

Semiconductor sensors have been around since the 1950's and today, every high energy physics experiment has one in its repertoire. In Lepton as well as Hadron colliders, silicon vertex and tracking detectors led to the most amazing physics and will continue doing so in the future. This contribution tries to depict the history of these devices exemplarily without being able to honor all important developments and installations. The current understanding of radiation damage mechanisms and recent R&D topics demonstrating the future challenges and possible technical solutions for the SLHC detectors are presented. Consequently semiconductor sensor candidates for an LHC upgrade and a future linear collider are also briefly introduced. The work presented here is a collage of the work of many individual silicon experts spread over several collaborations across the world.

Key words:
silicon sensors, pixel, tracking detectors, vertexing, radiation hardness, SLHC, RD50, 3D sensors, ILC, ISIS, CMOS, SOI, 3D integration
PACS: 29.40.Wk, 29.40.Gx

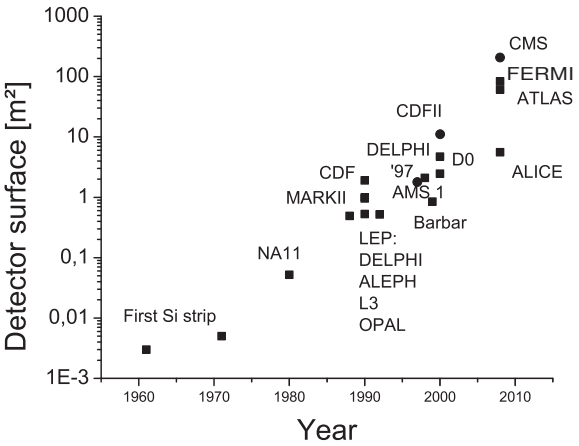

Figure 1: The evolution and usage of silicon as high energy physics detectors can be impressively shown by the increase in area during the last decades. [1]

1. Semiconductor Sensors – Past Present Future

In the past 40 years silicon detector's area increased constantly from a few square centimeters to 200 square meters as shown in Fig. 1 and 2. The diversity of detector challenges and subsequent solutions is vast and we are comfortable with our understanding of the detectors of the Present; the future is still uncharted territory and we will encounter many new surprises. During all the decades silicon detectors provided and will continue to provide precise momentum resolution, vertexing, *b* tagging, unprecedented accuracy in lifetime measurements, top quark identification, strong mixing background suppression - simply a lot of great physics!

2. Past

Semiconductor (large cell-type) sensors have been used since the 1950s for energy measurements. Precision position measurements were done until the 70s with emulsions or bubble chambers with limited rates and no trigger information! The traditional gas detectors were limited to 50 – 100 μm point resolution. High speed and high precision of silicon sensors enabled the tagging of second decay vertices and thus heavy quarks, to be used for the first time in the late 70's in fixed target experiments. After initial obstacles the use of silicon sensors took off – needed micro-lithography was initially very expensive; electronics miniaturization (transistors, ASICs) were not available; need of low noise amplifiers due to the small cell size. The *charm* of the *beauty* and capability of these devices enchanted many physicists and all LEP and TEVATRON experiments were equipped with silicon vertex detectors. At the time tasks were still bifurcated and silicon strip devices provided vertexing while gas detectors (mainly drift chambers and time projection chambers) were responsible for the outer tracking.

3. Present

Unprecedented detectors systems have been online since a decade, e.g. CDF II[2] and D0 detector; while recently the LHC detectors have been baptized by detecting their first proton collisions, in ATLAS, ALICE, CMS and LHCb. During the first brief data taking period at the LHC, all detectors proved their fabulous state of commissioning and detector understanding by re-discovering several particles in "no-time at all" [3]. I believe the main challenges of the LHC detectors have been the

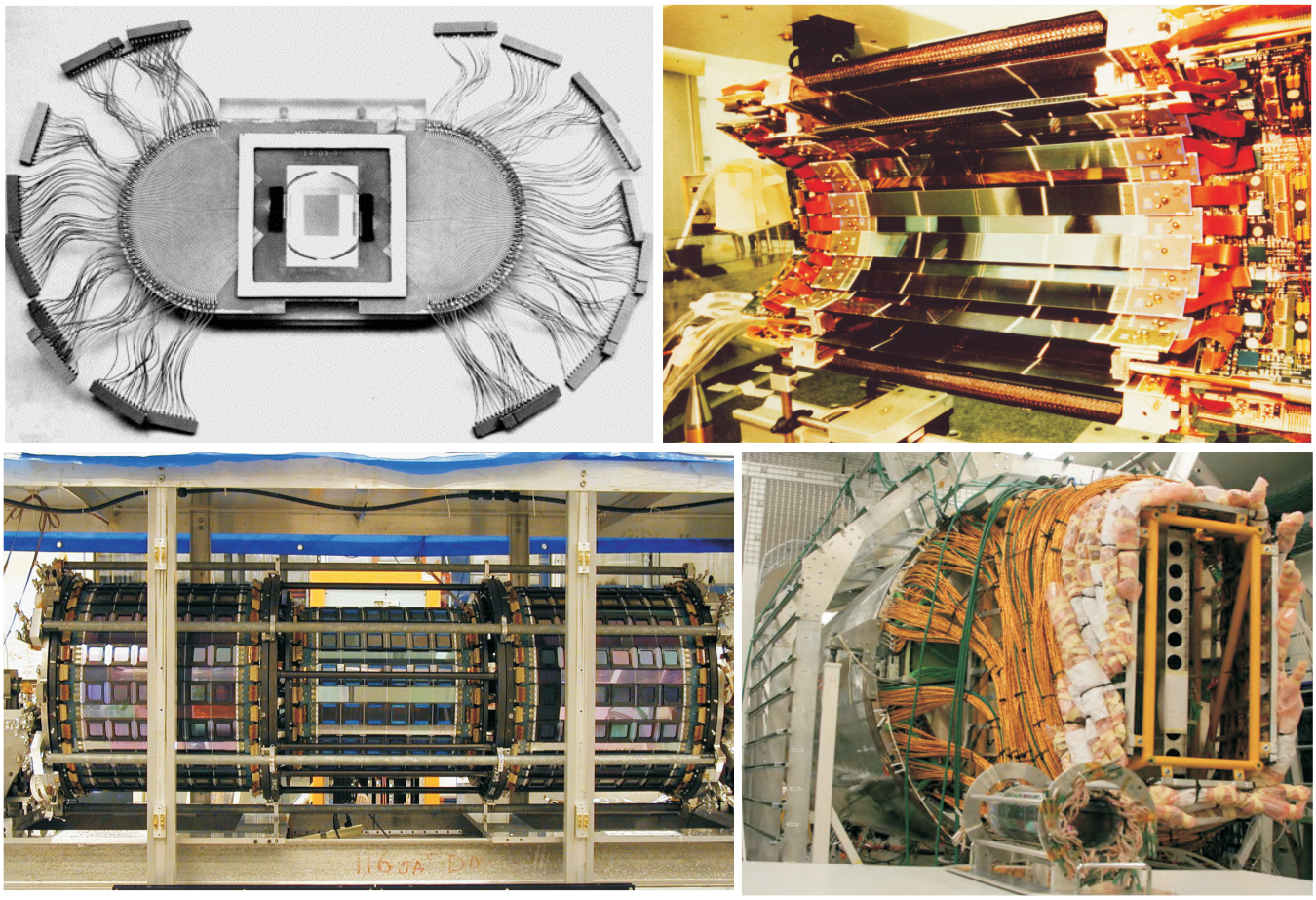

Figure 2: Picture of an NA11 sensor plane, an inner view of the DELPHI Micro Vertex Detector of 1994, the CDF Intermediate Silicon Layers detector of Run II and the packed CMS detector together with the OPAL silicon tracker. Area increased from 10^{-2} to 10^{0} to 10^{1} to 2×10^{2} m^2; the same evolution could be shown for number of channels, etc. [Courtesy CERN, FNAL]

complexity, the scaling up by more than one order of magnitude in size, construction period and deployment, besides the necessity of radiation hardness and the corresponding understanding. The CDF silicon strip tracker is responsible for vertexing and has a stand-alone tracking capability but is still complemented by an outer drift chamber. For the LHC, vertexing is done in the inner silicon pixel detectors while outer tracking is handled by silicon strip detectors (sometimes augmented by TPC and TRT). As chip technologies and module designs differ quite substantially between the LHC experiments, sensor technology is more constrained by the radiation hardness requirements, leading to single sided n-in-n diffused oxygenated floatzone DOFZ[4] sensors being used in the inner detectors and p-in-n FZ for the outer layers[1].

4. Excursion – Radiation Hardness

Tracking detectors are situated in the heart of the large HEP detectors, as close as possible to the particle interactions, suffering a harsh environment. Radiation fluence grows with increasing integrated luminosity and lower radius. Thanks to dedicated R&D collaborations, e.g. RD48 and RD50[5], plus enormous effort inside HEP detector collaborations, our current understanding of radiation damage and its time evolution is quite sufficient to design current TEVATRON and LHC experiments and operate them for many years.

4.1. Impact on Radiation Damage on Present Detectors

In principle we need to guarantee high efficiency, high resolution and low power consumption, but we are also interested in current, depletion voltage (V_{dep}), trapping, charge collection efficiency (CCE), signal to noise (SN) and strip parameters (inter-strip resistance, inter-strip capacitance, etc.). The current most used n-type FZ sensor material is very well understood with respect to bulk damage due to radiation (Φ_{eq}) and subsequent temperature dependant time evolution (annealing) and is extensively described in [1, 5, 6]. For n-FZ material, the fluence of different particles and different energies can be normalized via "non ionizing energy loss (NIEL)" calculations to 1 MeV neutron equivalent $1MeV_{eq}$"; damage from proton and neutron irradiation sums up. This is no longer true as soon as,

[1] ALICE will suffer less radiation and sensor technology is therefore more relaxed - pixel (p-in-n) + double sided strip sensors + SiDrift sensors

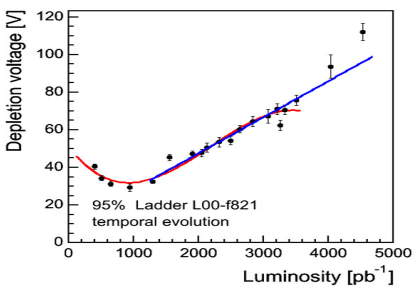

Figure 3: The evolution of depletion voltage of a CDF sensor during RUN II at the TEVATRON. The evolution is fitted by a polynomial 3rd order and the extrapolation by a linear fit. [2]

e.g. oxygen or carbon concentrations[2] become significant. Today, the main degrading parameters are current, effective doping ($N_{eff} \sim V_{dep}$) and trapping time (τ_{eff}).
Current increases with fluence $I \sim \alpha\Phi_{eq}$ and decreases for all silicon materials (n, p, FZ, MCz, oxygenated) with time. Current increase is the dominant damage item up to 10^{14} $1MeV_{eq}/cm^2$. It affects noise and power consumption.
V_{dep} is proportional to $|N_{eff}|$ while N_{eff} changes with Φ_{eq}. Different materials (n, p, FZ, MCz, EPI, DOFZ) behave differently with respect to different particles or their composition. For n-FZ only acceptors are building up, thus the effective doping concentration drops first to intrinsic[3] and then increases again. The annealing of $|N_{eff}|$ has two components with two different time constants, one beneficial where defects "recombine" and a reverse one, arising from a reconfiguration of defects into clusters leading to the build up of additional deep levels in the energy band. As a rule of thumb, depletion voltage evolution is the dominant damage item up to 10^{15} $1MeV_{eq}/cm^2$, defining power consumption and operability.
At the TEVATRON, the CDF experiment keeps us constantly up to date with the evolution of current and depletion voltages versus luminosity and extrapolations for the future operation parameters - see Fig. 3. Although direct comparisons with the Hamburg model[6] are not shown due to difficulties with accurate fluence determination, it can be deduced that nature is more kind than expected. It looks like long term operation and thus slow irradiation under bias voltage is less critical as a brutal 10 LHC years fluence equivalent in 10 minutes irradiation.

4.2. Additional Future Aspects of Radiation Damage Mechanisms

With higher fluences, around 10^{16} $1MeV_{eq}/cm^2$, trapping (trapping time) $\tau_{eff} \sim \Phi_{eq}$ becomes the dominant damage factor, where the signal (electrons and holes) due to ionisation is trapped before it reaches the readout electrodes ($\tau_{eff}(10^{15}\ n_{1MeV}/cm^2) = 2\ ns \Rightarrow x = 200\ \mu m$; $\tau_{eff}(10^{16}\ n_{1MeV}/cm^2) = 0.2\ ns \Rightarrow x = 20\ \mu m$). Trapping evolution due to irradiation differs for different materials (n, p, FZ, MCz, EPI, oxygenated) and also for the collected charge carriers, electrons or holes.

[2] As impurities or as wanted concentration, e.g. in diffused oxygenated material DOFZ

[3] Also called Space Charge Sign Inversion SCSI or simply inversion

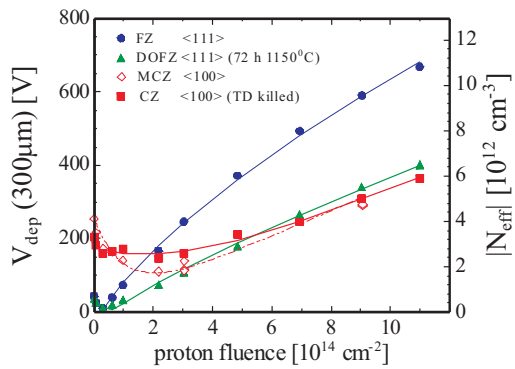

Figure 5: Cz and MCz do not exhibit the distinct point of space charge sign inversion. [7]

For future applications, with even higher radiation, the currently deployed detectors are not radiation hard enough. New materials and detector schemes had to be developed mainly within RD50 and LHC collaboration efforts. Fig. 4 gives a good overview of the current understanding of the signal achievable in different silicon sensors and materials. Clearly, it becomes difficult at fluences around 10^{16} $1MeV_{eq}/cm^2$ and above, while below current LHC technologies are mature enough. Already RD48 [8] proved the beneficial effect of oxygen concentration in the silicon material (DOFZ) with respect to depletion voltage evolution. This led to the exploitation of Czochralski material (Cz) and later to magnetic Czochralski (MCz[4]) where oxygen enrichment comes naturally during the melt process.
Radiation damage studies produced surprising results and in Fig. 5 no distinct SCSI point is present for these materials. After a long campaign of CV and TCT[5] studies, it became clear that with the new materials and with high fluences applied, one can no longer assume a linear electrical field with one single junction at one side. A double peak or double junction can be qualitatively explained by two opposite linear fields at both ends defined by different space charge regions at both ends and possibly a zero or constant field region in the middle. More quantitatively, fits suggest a parabolic field throughout the sensor volume. Often, with charge trapping, TCT signals from the injection side are trapped before they reach the other side and double peaks are smeared out; thus a trapping corrected TCT analysis is mandatory.
As a result, the depletion voltage parameter becomes a more abstract concept and for high radiation levels CCE or better SN becomes the more realistic and important parameter[6]. Furthermore, it has been realized that for some materials charged par-

[4] An applied magnetic field during the melt creates an electrical current distribution and an induced magnetic field. The active Lorentz force then dampens the oscillations in the melt.

[5] In a Transient Charge Technique TCT measurement the current slope represents the field and a sign change in slope indicates SCSI. Today we see a double peak thus a double junction.

[6] With higher and higher "depletion voltages" even above a possible operation voltage, the only important parameter is the collected charge at the amplifier

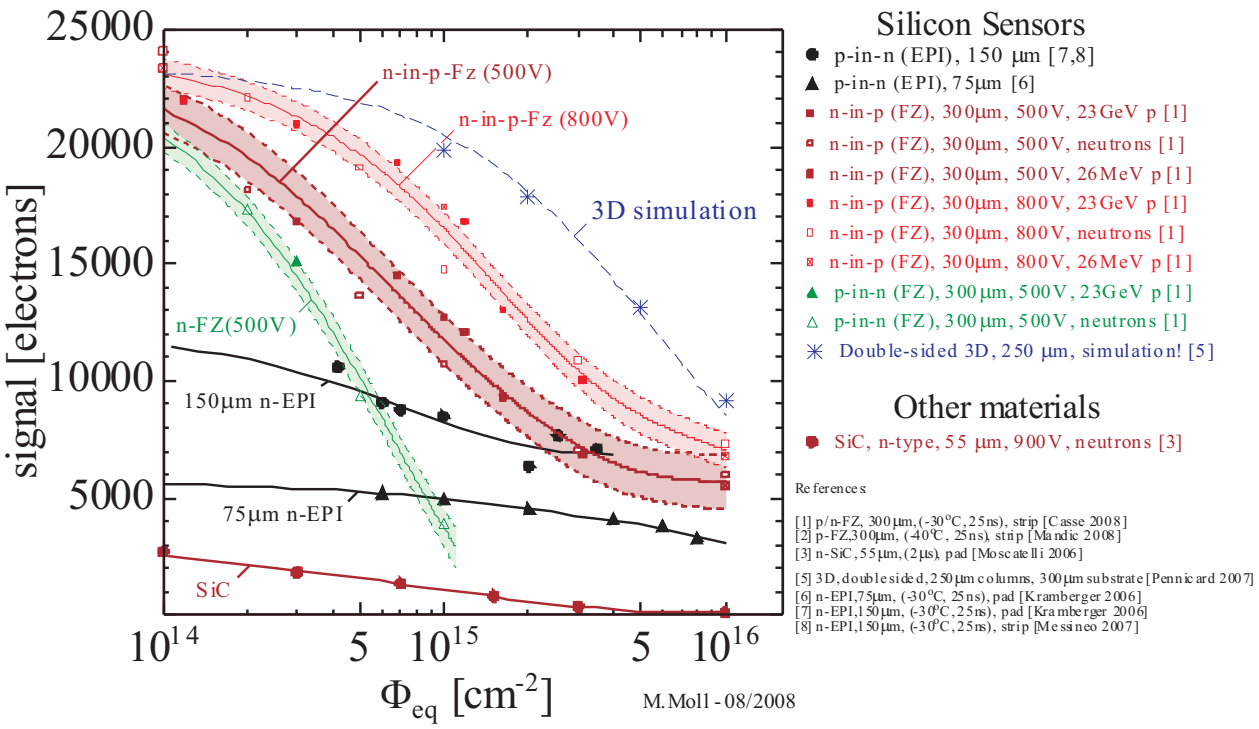

Figure 4: The plot compiles possible signals for different materials and different sensor schemes (planar, 3D) versus fluences. (Note: Measured partly under different conditions! Lines to guide the eye - no modeling)! [7]

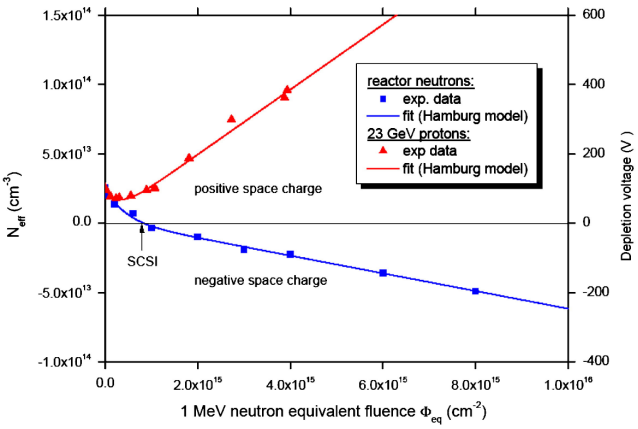

Figure 6: Change of N_{eff} in EPI-DO material versus irradiation with different particles. Acceptor introduction is enhanced for neutrons irradiation, similar to n-FZ material, while protons generate mainly donors. In the corresponding study the deep level states have been identified with the Thermal Stimulated Current TSC method. [16]

ticles introduce distinctly different defects than neutrons. Fig. 6 shows for EPI-DO the introduction of negative space charge after neutron irradiation with the corresponding SCSI. Instead for protons, donor generation is enhanced (positive space charge) and therefore no SCSI is observed.

In the case of n-FZ sensors, both neutron and proton radiations introduce predominantly p-type defects. In the case of n-MCz, the neutrons introduce mainly p-type defects while charged particles mainly n-type defects - a clear violation of the NIEL hypothesis. This particular feature of the n-MCz silicon can have a favourable consequence on the degradation rate of the electrical properties of the detectors when the damage is due to a comparable mix of neutron and charged hadrons because the n and p-type radiation induced defects can partially compensate. To test this effect, n-in-n FZ and n-in-n MCz detectors have been irradiated with neutrons only, 25 MeV protons only and with an equal mix of neutrons and 26 MeV protons to a total dose of $1 \times 10^{15} n_{eq} cm^{-2}$. Fig. 7 shows the CCE(V) measurements of these devices and confirms the compensation effect. The two n-FZ detectors exhibit almost identical CCE(V) characteristics after the neutron, proton and mixed irradiations, while the n-MCz shows a faster rise of the CC(V) in the case of mixed irradiation relative to the neutron and proton irradiations. Obviously, the "old" NIEL mantra is not really adequate anymore for the new materials! Charged particles damage differently, protons may even compensate for neutron damage. NIEL is still useful for scaling between different proton energies and to evaluate the leakage current after hadron irradiation. But, while new materials seem to be more radiation hard, a complete evaluation of each material must be done separately for neutron, proton and mixed irradiation. This is especially important for the upcoming SLHC studies.

4.3. Microcosmos – Macrocosmos

With respect to these introduction of acceptors and donors, the RD50 and WODEAN[10] collaborations are investigating the correspondence of microscopic defects and macroscopic parameters. One example is presented, where levels H116K, H140K, H152K can be identified being responsible for reverse annealing. These levels do not form with γ radiation and are

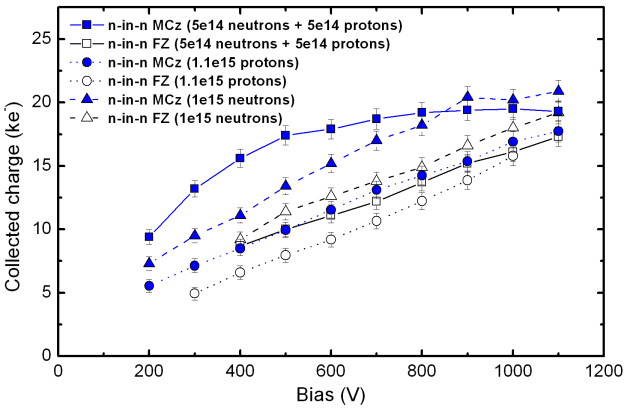

Figure 7: Charge Collection Efficiency of MCz and FZ detectors after a total dose of $1 \times 10^{15} n_{eq} cm^{-2}$ obtained with neutrons only, 26 MeV protons only or mixed (equal dose of neutrons and 26 MeV protons) irradiation. The CCE of the mixed irradiation is roughly the average of the proton and neutrons for the FZ sensors, while mixed irradiation improves the CCE at low bias voltages for the MCz sensors relative to only neutron or proton irradiations, indicating a /compensation/ effect (with decrease of the $|N_{eff}|$) between the neutron and proton induced damage. [9]

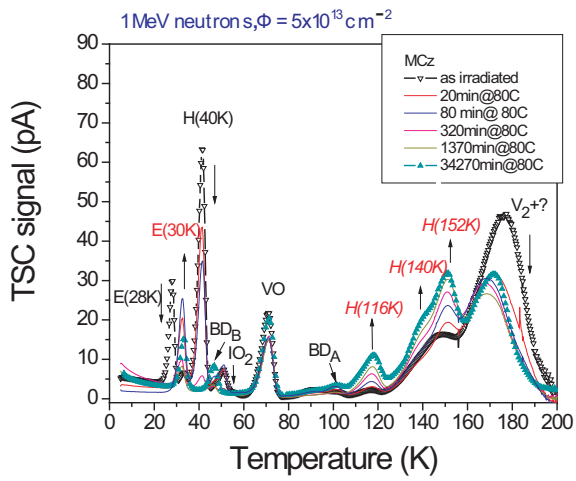

Figure 8: Thermally Stimulated Currents Method scans were done after each annealing step. The rise of the microscopic levels H116K, H140K, H152K can be observed after each annealing step. [11]

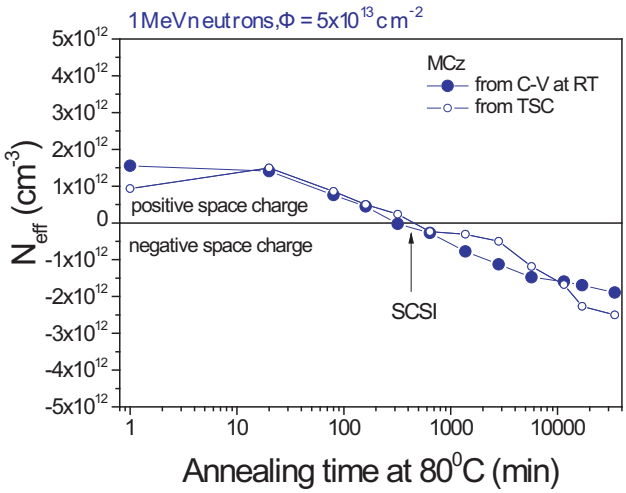

Figure 9: For each annealing step, the depletion voltage was determined by means of a C-V characteristics and a TSC scan. The change matches the rise of the defect levels H116K, H140K, H152K (see Fig. 8) [11]

therefore cluster defects. The concentration of these levels increases with longtime annealing corresponding with negative space charge build-up (N_{eff} change). Figure 8 shows the Thermally Stimulated Currents Method (TSC) to determine the defect level concentrations while Fig. 9 shows corresponding the N_{eff} change.

4.4. Radiation Hardness of Different Materials at High Fluences

Apart from this, numerous studies have been conducted, mainly inside the RD50 framework, to evaluate the radiation hardness of different sensor technologies, e.g. planar p-in-n, n-in-n, n-in-p processed in FZ, EPI and MCz material resulting in applications recipes for the possible future LHC upgrade. Fig. 10 shows a representative example of CCE results of different materials irradiated with 25 MeV protons to several fluences. All in all, the CCE results favor n-strip (electron) readout. Obviously the collection of electrons is favored but for a final implementation all factors have to be taken into account, e.g. noise and the larger Lorentz angle. Fig. 11 teaches us that at very high fluences trapping becomes the dominant damage factor (reducing signal) and different particle radiation result in the same effective CCE.

4.5. Charge Amplification

In the last two years different groups reported higher CCE after irradiation than before, completely incompatible with any trapping model. In several cases more charge per volume has been recorded than a MIP deposits due to ionization. Fig. 12 shows three examples hinting at a charge *amplification* mechanism. It is now of utmost importance to evaluate if the charge amplification is really the wished modus operandi for silicon

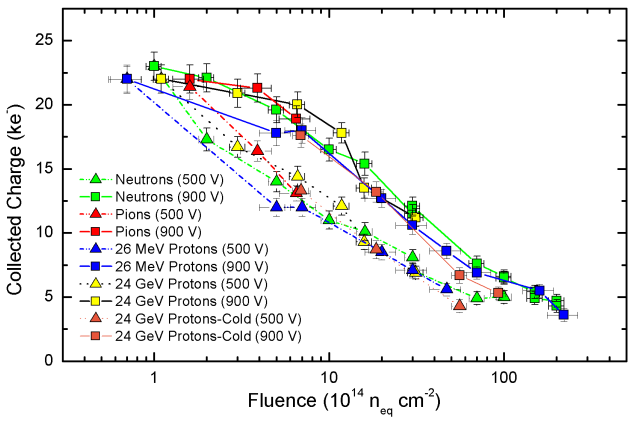

Figure 11: The plot shows CCE for n-in-p FZ strip detectors vs. fluence of different particles. At high fluences trapping becomes the dominant factor and damage becomes almost particle independent. The knee in the most right tail looks even a bit too high and could be a hint to charge amplification. [12]

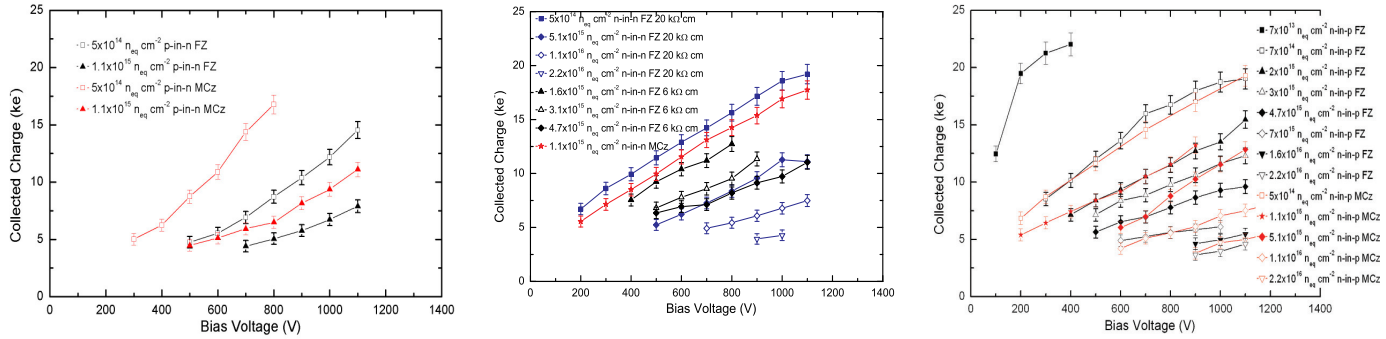

Figure 10: The plots show from left to right CCE of p-in-n, n-in-n and n-in-p planar sensors irradiated to several different fluences with 25 MeV protons (KIT, Cyclotron). The results can be summarized, that CCE for p-in-n is insufficient for $\Phi > 10^{15}$ while it was possible to even measure a small signal above $\Phi = 2.2 \times 10^{16}\ n_{1MeV}/cm^2$ for n-in-n sensors. It can also be said, that n-MCz is much better than n-FZ for proton irradiation. Similar good CCE results are shown for n-in-p sensors, while here p-MCz is not substantially better than p-FZ. All in all the CCE results clearly favor the use of n-strip (electron) readout. [12]

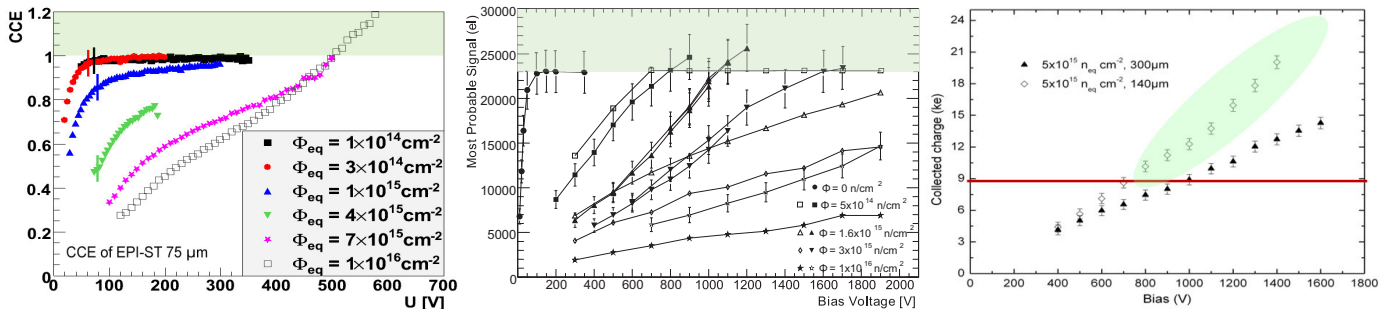

Figure 12: Several groups claim to collect more charge after irradiation than before and even more charge than a MIP can deposit in the given material volume. The first plot (J. Lange, HH [13]) shows a higher signal in n-EPI material after irradiation, the second (I. Mandić, Ljubljana [14]) a higher signal in p-FZ sensors after neutron irradiation (reactor Ljubljana). The last (G. Casse, Liverpool [15]) shows a higher signal in a p-FZ 140 μm thin sensor with respect to the 300 μm thick sensor and also with respect to charge deposited by a MIP in the corresponding volume (after $5 \times 10^{15}\ n_{1MeV}/cm^2$ with 25 MeV-p). Clear signatures of charge amplifications have been identified.

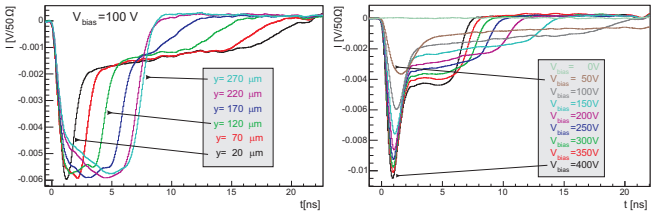

Figure 13: Edge TCT, a novel tool to achieve a deep understanding of charge propagation was developed in the Jožef Stefan Institute, Ljubljana, Slovenia. Infrared laser light shines from the side allowing dedicated charge deposition per unit depth. The left figure show the different TCT signals per depth in a non-irradiated n-in-p FZ sensor (V_{bias} = 100 V); y=270 μm is situated near the backplane and y=20 μ near the strip region. The initial peak represents the collected electrons and the long tail comes from the drift of holes. The shortest signal can be seen for y=220 μ, where electron and holes have an equal drift time. In the right figure, a bias scan at y=20 μ has been done. The second peak in the induced current is getting shorter with voltage as well as the electron peak is getting higher. The system allows very detailed studies. [18]

sensors in the HEP environment. How is the leakage current and the noise affected, what is the resulting effective signal to noise? Further dedicated studies are needed.

A new tool developed in the Jožef Stefan Institute in Ljubljana sheds new light on the amplification mechanism - Edge TCT [18]. Combining the TCT with the "grazing" signal method, infrared laser light shines into the sensor from the side. After preparation (cutting, polishing) the side of a sensor parallel along a strip, light can be injected perpendicular to the strips therefore shining into defined regions with respect to volume depth and illuminating homogeneously several strips. In this configuration no weighting fields for individual strips need to be taken into account; strips and neighbors experience the same charge without disturbing the real field configuration. Fig. 13 shows a charge deposition versus depth scan. This is more effective and offers much more information than front or back face light injection only. The detail description of this impressive tool and the possible analysis is not in the scope of this proceeding but some highlights will be listed.

The edge-TCT allows the determination of the "velocity profile", "trapping time", "electrical field" and "charge collection profile". Fig. 14 exhibits a direct indication for charge amplification, the second time-delayed peak in the current pulse can be explained by electron-hole creation at the very high electrical field at the strip face. The corresponding holes from the amplification process have been excited later than the original ones from light injection and then drift from the strip region to the back side. A second observation by this method, not detailed here, is that the velocity and electrical field profiles do not give a consistent picture without charge amplification. During a voltage scan, it has been identified that the charge collection correlates with the leakage current; see Fig. 15. The mechanism works for electrons coming from signal as well as from dark current. To summarize, it has been proven that planar sensors exhibit a much higher signal than trapping extrapolations at lower fluences suggested and even higher than ionizing MIP particles deposit; simply increasing the bias voltage seems to help. On the other hand it has to be proven that amplification in a solid state detector is really a controllable correct operation

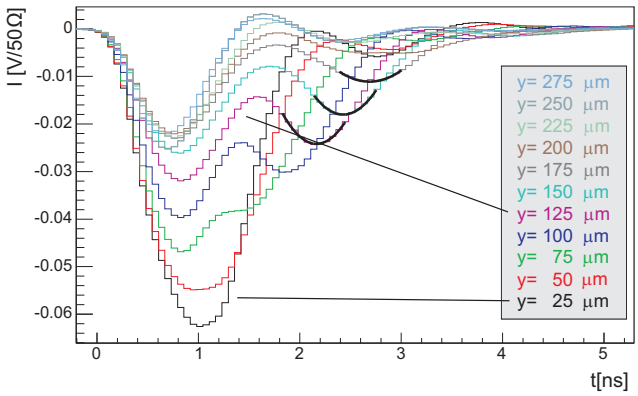

Figure 14: The second peak in the hole tail is evidence of charge amplification in n-in-p sensors in the high E-field strip region. As explained the tail corresponds to holes from the initial laser light, the additional peak in the tail represents additional holes created at a later time together with electrons in the amplification process when the electrons reach the high field strip region; the holes then need to drift to the back. [18]

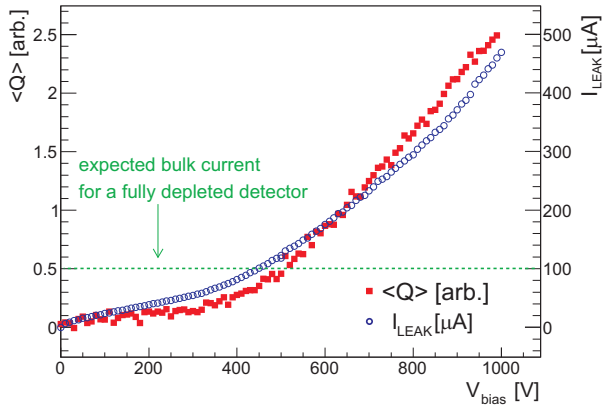

Figure 15: The charge profile, a derived value, corresponds to an increased leakage current exceeding the expected values for the fully depleted sensor. [18]

model.

4.6. Recent Annealing Studies

Besides the evolution with fluence also the annealing behavior of the new materials and detector schemes must be explored thoroughly; e.g. to answer the question if two different technologies in one detector would need different temperature maintenance scenarios. Again many groups are investigating this topic and two detailed studies are considered here. In Fig. 16 it is shown, that current as well as the corresponding shot noise and power consumption decreases at elevated temperatures, while the signal is more or less stable and constant [17]. This has been observed for n-in-p sensors from two vendors for several fluences (neutron & proton irradiation), while CCE degradation with annealing was still present for p-in-n sensors. The study suggests that sensors should be kept warm during maintenance to reduce power consumption without SN degradation.
Another study [18] also shows a practically constant SN but an increase in signal, noise and current, ergo, power consumption. The study suggests that fields are changing with an onset time for charge amplification. Further studies are needed to understand all the different effects.

4.7. Summary and conclusion of radiation hardness excursion

Today, the radiation damage mechanisms for n-FZ are understood on a detail level, the evolution of sensor parameters can be followed (TEVATRON) and predicted (LHC). Also macroscopic values can be correlated with specific deep levels in the band gap, e.g. current and N_{eff}, and trapping is not an issue at these fluence regimes. For the future, with all the new materials and sensor schemes, new surprises have been encountered. SCSI has been relieved by a double junction field configuration, V_{dep} is a more and more abstract concept, while SN or better efficiency and resolution (and also power) are the more important parameters. Every material needs evaluation with proton, neutron and mixed irradiation separately to understand the different damage mechanisms - damage addition or compensation. Recipes for the future SLHC detectors exist, but there are still unanswered questions and challenges: Will we be able to exploit/tame the amplification mechanism? What will be the best maintenance scenario?

5. Future

It is beyond the scope of this article to detail or even mention all planned future detectors, only some examples (SLHC, *b*-factories, ILC) will be described. Also some novel sensor concepts will be introduced.

5.1. Super Large Hadron Collider

The LHC will deliver a peak luminosity of $10^{34} cm^{-2} s^{-1}$ of 14 TeV p-p collisions summing up to an integrated luminosity of 500 fb^{-1}. Physics cases, like Higgs couplings, and new physics hopefully awaiting discovery, such as SUSY spectroscopy, would profit from even higher statistics. As a matter of fact, plans are shaping to increase luminosity to $10^{35} cm^{-2} s^{-1}$ eventually yielding an integrated luminosity of $\sim$ 5000 fb^{-1} in a later LHC upgrade stage: the Super-LHC or SLHC. Generally the silicon trackers would not survive the much higher radiation environment of the SLHC and current channel granularity could not cope with the much increased occupancy (up to 400 events per bunch crossings are envisaged). Upgrade planning foresees two stages[7], where in the first one the most inner detectors are to be upgraded and in a later stage complete new trackers will be installed. Fig. 18 displays the two main concepts for ATLAS and CMS. While ATLAS develops an additional insertable most inner pixel b-layer IBL, CMS plans to exchange the three barrel - two endcaps pixel device with a four barrel - three endcap low material budget pixel device. LHCb plans to fully exchange its VELO detector with a pixel device. ATLAS and LHCb are investigating planar, 3D sensors and diamond detectors, while CMS intend to use the current planar n-in-n technology. Many new infrastructure strategies are under discussion and already in an advanced planning stage, e.g. CO_2 cooling, DC-DC or serial powering, new chips, etc.

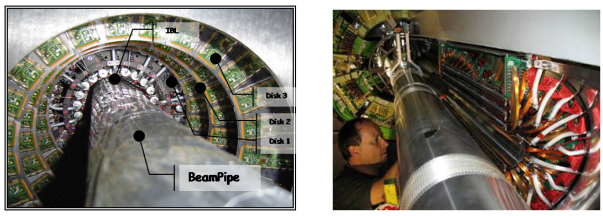

Figure 18: LHC PHASE I Upgrade strategy of ATLAS and CMS: ATLAS plans to insert an additional pixel *b*-layer IBL (left) to compensate degradation in the current inner pixel layer; CMS plans to exchange the full pixel detector with a new one. The half-shell concept allows CMS to easily exchange its pixel device in the order of days/weeks; tested in 2009 during the shutdown (right).

Phase II detectors are even less well defined, where the main challenges will be radiation hardness, occupancy and integration. ATLAS design plans indicate a fine granular pixel detector for the innermost layers followed by short strip sensors and further out long strip layers. According to the current studies n-in-p FZ sensors mounted in stave and petal like design are the baseline concept. CMS has not yet decided on a final layout nor chosen a final sensor concept but has identified a novel requirement, which is to provide tracker data (cut on p_T) to contribute to the first level trigger[8]. This requires a local correlation between sensors spaced by a few millimeters, so called p_T modules. Here even new 3D sensor-electronics integration schemes are under discussion along with more conventional correlation layers connected via bump bonding. It should be mentioned that the bifurcation will reach a new level: vertexing is done by fine pixel sensors and tracking by long pixel or short strips, all realized in silicon.

[7] With new machine schedules all planning is in the motion also affecting detector upgrade plans.

[8] maintain the 100 kHz rate for compatibility with existing sub-detector systems while increasing the trigger decision latency by only a few μs

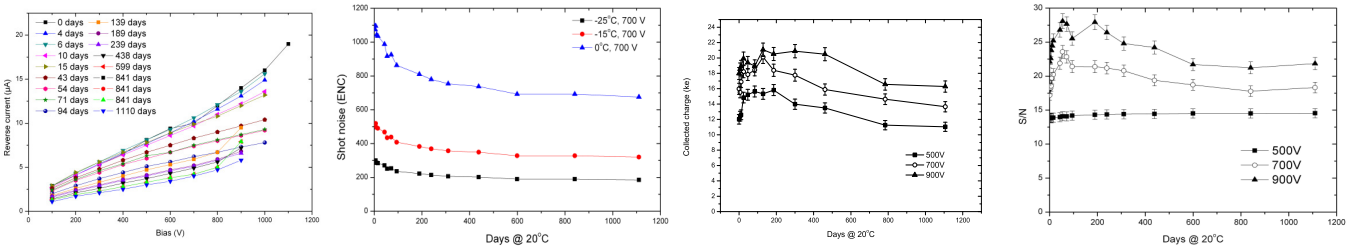

Figure 16: The figures present (from left to right) the annealing of dark current, shot noise, collected charge and signal to noise for n-in-p FZ sensor after 10^{15} n_{1MeV}/cm^2 25 MeV protons. [17]

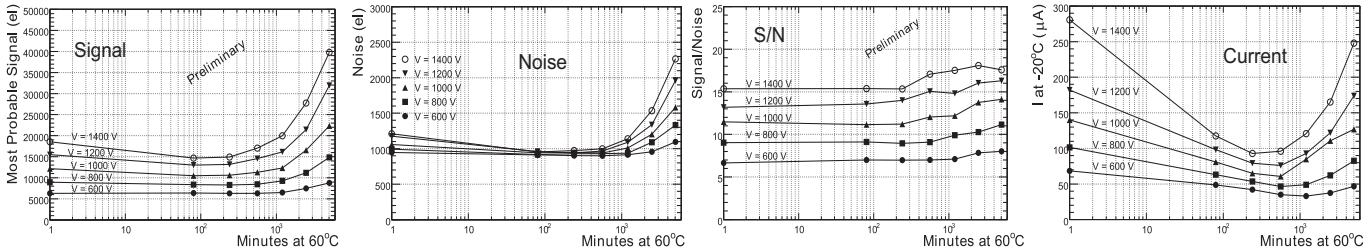

Figure 17: Annealing and amplification of n-in-p FZ sensors. Current, signal and noise increase in the regime of reverse annealing, this could possibly be explained by the on-set of charge amplification. The signal to noise ratio slightly increases. [18]

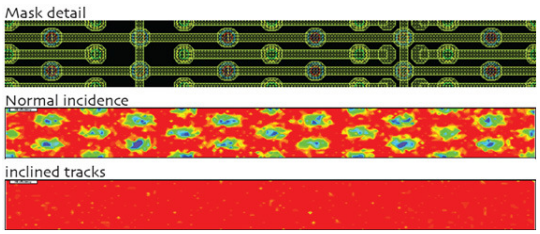

Figure 19: Efficiency in 3D sensors increases to 99.8% for inclined tracks. [20]

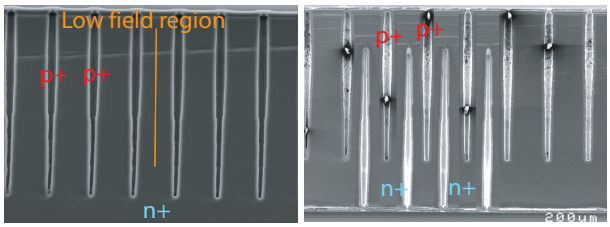

Figure 20: The 3D single column type STC (left picture) suffer from a low field region between columns due to lateral depletion. 3D double-sided double type columns DDTC (right picture) are more complicated but have a full field over the whole volume. [Courtesy of CNM]

5.1.1. 3D sensors

It has been mentioned before that trapping is the dominant damage after high irradiation and increasing the sensor thickness does not help to gather more charge. All LHC experiments are investigating the 3D concept[19]. In the 3D concept, electrodes are realized as narrow columns along the detector thickness with a diameter around 10 μm and a spacing of 50 – 100 μm. The deep reactive ion etching DRIE can also be used to etch trenches and allow the production of edgeless sensors. This scheme reduces collection time and the collection distance becomes equal to the column distance, therefore trapping is substantially reduced. Sensors seem to be radiation hard up to $n \times 10^{16}$ $1MeV_{eq}$. The lateral depletion results in low depletion voltages independent of the sensor thickness being large to collect large signals. As a caveat, the high channel capacitance and the inefficiency inside the columns has to be mentioned. Recently, small modules have been built and the concept of these devices have been proven in test beams and with laser tests. Signal formation and resolution is similar to planar sensors and efficiency recovers up to 99.8% for inclined tracks, see Fig. 19. The new 3D double-sided double type columns DDTC design (see Fig. 20) overcomes the low field region in the middle of columns in the STC design. It has to be mentioned also that hints for charge amplifications have been spotted for 3D sensors [20].

5.2. Future Linear Collider

The tracking detector requirements for a future linear collider or in general an e^+e^- machine are completely different to the SLHC ones. For the International Linear Collider, vertex detectors have to be able to distinguish c-from b-quarks. The impact parameter resolution should be $\sigma_\phi \approx \sigma_z \approx 5 \bigoplus 10/(psin\Theta^{3/2})\mu m$ requiring a point resolution of 1-5 μm. Tracking requires a superb momentum resolution of $\Delta(1/p_T) = 5 \cdot 10^{-5}/GeV$. The transparency must be $\sim 0.1\% X_0$ per layer equal to max 100 μm of silicon. The transparency requirement implies directly a low mass structure, no cooling pipes and thus a very low power system implementation. The readout electronics are designed with a power pulsing feature to utilize the train/bunch structure and be inactive most of the time. The possible candidates under development are numerous and include (1) **C**harge-**C**oupled **D**evices (CCDs), CPCCD (**C**olumn **P**arallel **CCD**s), (2) **M**onolithic **A**ctive **P**ixels MAPS based on CMOS technology,

(3) DEPFETs (**DE**pleted **P**-channel **F**ield **E**ffect **T**ransistor), (4) SOI (**S**ilicon **o**n **I**nsulator), (5) ISIS (**I**mage **S**ensor with **I**n **S**itu **S**torage), (6) **H**ybrid **A**ctive **P**ixel **S**ensors (HAPS) and 3D integration concepts. The devices for the ILC come in several flavours with some specific implementations and also some technology combinations. Standard CCDs as used in digital cameras are not fast enough, proposed column parallel readout CPCCD helps even more with shorter columns in the **S**hort **C**olumn **C**harge **C**oupled **D**evice (SCCCD) design, where a CCD layer and a CMOS readout layer is bump bonded together. Chronopixels are CMOS sensors, with the capability to store the bunch ID (time). ISIS sensors combine CCD and active pixel technology, a CCD like storage cell together with CMOS readout implemented. Also **F**lexible **A**ctive **P**ixel (FAPs) integrate storage cells in the traditional MAP cells. **F**ine **P**ixel **CCD** FPCCDs are under discussion to decrease occupancy. To summarize, the different varieties of CCDs, DEPFET, MAPS and SOI are designed to read out every 50 μs, while ISIS and FAPS store signal in cell memory and will be read out in the 199 ms between trains. Also FPCCDs and Chronopixels are designed for in-between train readout. Recent developments of MAPS, ISIS, SOI and DEPFET technology will be briefly described the next sections.

5.2.1. Monolithic Active Pixels aka CMOS

MAPS/CMOS sensors have been introduced 1999 as early R&D. Sensor volume and electronics share the same substrate, in-pixel processing is possible (NMOS only), e.g. amplification, sparsification, column parallel architecture with digitization at column level. The charge is generated in the epitaxial layer and reaches the electrodes by thermal propagation ($\sim 100e^-$); no depletion voltage is applied in the standard configuration. The scheme allows very high granularity with resolution down to 2 μm at very low noise. Sensors are very thin by design with a very fraction of X_0. Today, there is a huge diversity of sensors. Many groups are involved for many different applications, e.g. the Mimosa chips exists in version 26 (0.35 μm). The Current generation is radiation tolerant up to $n * 10^{13} n/cm^2$.
Groups are developing "high" ($\sim$ 60 V) voltage CMOS technology devices to allow depletion of the EPI-layer thus collecting $\sim 1000e^-$ [21]. Another group (LEPIX) plans a MAPS submission for use in the future SLHC environment in standard very deep submicron CMOS technology (90 nm) to increase radiation. Dedicated work is ongoing on the development of thin, fully depleted MAPS with binary readout based on vertical 3D integration of heterogeneous CMS layers - digital parts on top of analog circuitry [22]. MAPS are used in standard digital cameras, the EUDET telescope and a detector for STAR @ RHIC (commissioning 2010). MAPS are candidates for ALICE, ILC, FAIR and SuperB.

5.2.2. In-situ Storage Image Sensor ISIS

The ISIS design consequently combines CCDs, active pixel transistors and CMOS edge electronics in one device. The signal charge (raw) is collected under an array of photogates into a buried channel next to the pixel. Charge is then transferred to an in-pixel register 20 times (20 kHz) during the ~1 ms short train. After a charge to voltage conversion, the signal is leisurely readout in the 200 ms long 'in-between-train' quiet period. The system shows an excellent noise performance and is immune to RF pickup during the bunch train. Finally, 1 MHz column-parallel readout at end of a ladder is sufficient, with on-chip edge logic for cluster finding, centroid determination and data sparsification. The ISIS schematic is presented in Fig. 21. A second version, ISIS2 processed in 180 nm, has recently been evaluated [24].

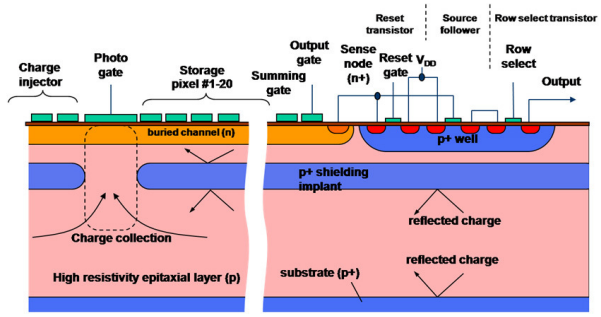

Figure 21: Scheme of the ISIS detector. ISIS consequently combines CCDs, active pixel transistors and CMOS edge electronics in one device.[24]

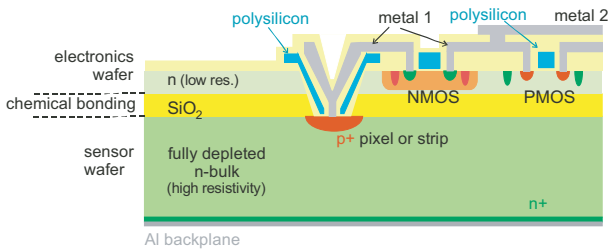

Figure 22: The schematic of Silicon On Insulator SOI sensor is shown. The low resistivity CMOS electronics wafer is separated by a thin insulation layer to the high resistivity sensor wafer, which then can be operated in a depleted mode. The two wafers are chemically bonded and contacts to readout implants are established by etching through the insulator.

5.3. Silicon On Insulator SOI

Silicon On Insulator has been introduced 2003 for the SUCIMA project by ITE Warsaw. Today it is a research topic of several groups worldwide with the plan to introduce it for the Belle-II, ILC and SLHC project [25]. The scheme is presented in Fig. 22. The goal is the integration of the electronics low resistivity wafer with a high resistivity sensor by chemical wafer bonding. The separated electronics part can then utilize NMOS and CMOS transistors allowing in-pixel processing, low power, high speed, while the sensor volume can be fully depleted to allow a high and fast signal. The high granularity allows high resolution. A point resolutions of down to 1 μm have been achieved. The radiation hardness asks for low feature sizes at the electronic side, where samples with 150-200 nm have been processed. A remaining problem is the back-gating effect, where the sensor bias voltage effects the analog transistor functions.

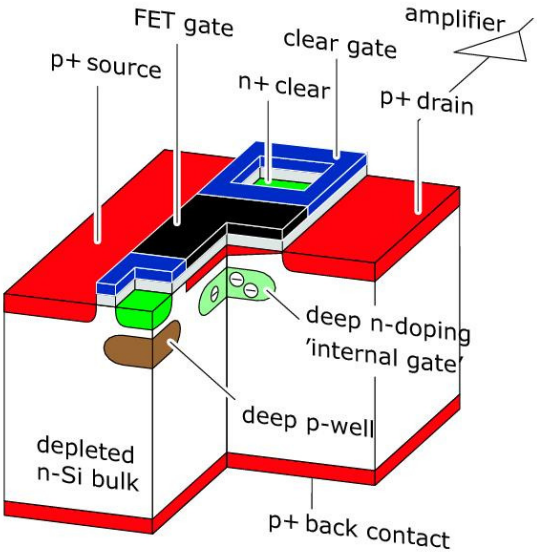

Figure 23: Scheme of one DEPFET cell. [23]

5.3.1. DEPleted Field Effect Transistor DEPFET

DEPFETs are candidates for the ILC, MIXS, NEWTON, etc. and are the baseline choice for the Belle-II vertex detector. Current DEPFET sensors have a superb signal to noise ratio of 120 to 220 and a point resolution of 2-3 μm combined with a low power consumption. These devices are sensitive even when they are in the OFF state. The main feature is the in-pixel amplification, where the charge generated by ionizing particles collected at the internal n-gate, modulates the source/drain current, the signal. The scheme is shown in Fig. 23. The resistivity bulk is fully depleted guaranteeing a fast charge collection. The amplification also allows the use of very thin devices ($\sim 50\,\mu m$) to achieve a low material budget. It has to be mentioned that relatively high voltages ($> 10V$) are necessary to clear the internal gate from time to time.

5.4. 3D Integration

Industry is very much interested in the development of a 3D chip, where separate layers on top of each other have different functionality and even different technologies, e.g. memory, digital electronics, analog electronics, optoelectronic devices and waveguides and maybe even MEMS interconnected to each other in one monolithic circuit. This would help industry to reduce the interconnect length, thus improve speed, reduce interconnect power and reduce crosstalk. It also decreases chip footprint size, which would also be very much of interest to the miniaturization efforts of HEP. In HEP the main interest is to include the sensor, the analog IC and the digital IC into a single monolithic device connected with silicon through vias (TSV). Implementation studies are ongoing in the MAPS sector [22]. Also for the newly required p_T modules by CMS, 3D integration could help a lot. One can imagine a sandwich of sensor - readout electronics - a thick interposer/correlator - readout electronics - sensor fully implemented in a monolithic structure. Developments are ongoing and plans exist mainly for detectors for ILC and SLHC. This is the challenge today: to improve miniaturization a further step while increasing functionality and decreasing power and noise. If successful, the new development can solve many problems and allow artistic architectures of today but more and more sensor construction will then be done directly and fully by industry.

6. Conclusion

Semiconductor sensors have been operated since the 50ties very successfully. They matured during the LEP era and are instrumented in every current HEP detector. The new most ambitious developments are candidates for ALL future detectors. The radiation damage mechanisms are well understood for sensors instrumented in the TEVATRON and the LHC experiments - the problem of leakage current and high depletion voltages is under control. For the future detectors we have to find solutions to trick the trapping, e.g. by high bias voltages or 3D sensors. We have to evaluate if we can reliably operate solid sensors in the charge amplification regime. Material and device engineering of the last years provided us with recipes for the SHLC detectors. Planar sensors, especially with n-strip readout are viable options for all but the innermost layers. Oxygen is very beneficial, DOFZ and MCz show higher radiation tolerance especially for charged particle irradiations. Higher voltage, ergo, higher fields and faster readout helps. The first modules of 3D and diamond sensors, candidates for the most inner layers, exist and have proven their potential in recent test beams.
The integration of sensors and electronics is becoming more and more interesting for SLHC and even more for a linear collider. HAPS, FAPS, MAPS, CCDs, DEPFET, SOI, ISIS the number of acronyms is already too large for me to keep in mind. First baby steps are ongoing to utilize 3D electronic integration, where the idea is to stack sensor, analog and digital layers on top of each other connected via silicon through vias. This new kind of integration has the potential to herald a new era of silicon tracking detectors.

The diversity of silicon detectors deployed in all current high energy experiments is only exceeded by the incredible number of new front-edge technology developments ongoing right now. I'm very lucky to participate in such a lively and friendly environment of history, detector operation and ground-breaking R&D.

References

[1] Evolution of Silicon Sensor Technology in Particle Physics; Series: Springer Tracts in Modern Physics; http://www.springer.com/series/426, Vol. 231 (2009), ISBN: 978-3-540-25094-4

[2] Serge Jindariani, Longevity Studies in the CDF Silicon Detectors, these proceedings

[3] M. Sitta, "The Silicon Drift Detector of the ALICE experiment"; C. Kuo, "First results on the performance of the CMS Preshower Detector"; C. Parkes, "Results from the first LHC beam reconstructed tracks in the LHCb Vertex Locator"; M. Weber, "First Alignment of the Complete CMS Silicon Tracker"; C. Troncon, "Commissioning of the ATLAS Pixel Detector with cosmic ray and beam data"; W. Johns, "CMS Pixel Detector"; these proceedings

[4] G. Casse, M. Glaser, Glaser, F. Lemeilleur, A. Ruzin, M. Wegrzecki, "Introduction of high oxygen concentrations into silicon wafers by high temperature diffusion", NIM A 438 (1999) 429-432.
[5] http://www.cern.ch/rd50
[6] M. Moll, Radiation Damage in Silicon Particle Detectors, Universität Hamburg, DESY-THESIS-1999-040, 1999
[7] M. Moll, Recent advances in the development of radiation tolerant silicon detectors for the Super - LHC, presented at 11th ICAPTT conference, Como, 5-9.Oct.2009
[8] G. Lindstrom et al., "Radiation hard silicon detectors developments by the RD48 (ROSE) Collaboration", NIM A466 (2001)308-326.
[9] A. Affolder, P. Allport, G. Casse, Collected charge of planar silicon detectors after pion and proton irradiations up to $2.2 \times 10^{16} n_{eq} cm^{-2}$, $NIMA$ (2010), doi:10.1016/j.nima.2010.02.187.
[10] WODEAN project (initiated in 2006, 10 RD50 institutes, guided by G.Lindstroem, Hamburg)
[11] I. Pintilie, E. Fretwurst, G. Lindstrm, A. Junkes (e.g. Appl. Phys. Lett. 92, 024101, 2008)
[12] A. Affolder, P. Allport, G. Casse, Collected charge of planar silicon detectors after pion and proton irradiations up to $2.2 \times 10^{16} n_{eq} cm^{-2}$, NIM A (2010), doi:10.1016/j.nima.2010.02.187.
[13] J. Lange et al., Charge collection studies of proton-irradiated n- and p-type epitaxial silicon detectors, 11th ESSD, 2009, to be published
[14] Igor Mandić et al., Observation of full charge collection efficiency in heavily irradiated n+p strip detectors irradiated up to $3 \times 10^{15} neq/cm^2$ NIM A 612 (2010) 474-477
[15] G. Casse et al, Enhanced efficiency of segmented silicon detectors of different thicknesses after proton irradiations up to $1 \times 10^{16} neqcm^2$, NIM A, doi:10.1016/j.nima.2010.02.134
[16] I. Pintilie et al, Radiation-induced point- and cluster-related defects with strong impact on damage properties of silicon detectors, NIM A 611, Issue 1(2009) 52-68
[17] G. Casse, New Operation Scenarios for Severely Irradiated Silicon Detectors, PoS Vertex 2009
[18] I. Mandić and G. Kramberger, talks at the 15th RD Workshop 2009 in Geneva http://rd50.web.cern.ch/rd50/15th-workshop to be published
[19] Introduced by S.I. Parker et al., NIMA 395 (1997) 328
[20] P. Hansson, Recent Test Beam Results of Radiation Hard 3D Silicon Pixel Sensors & G. Pellegrini, Charge collection efficiencies of 3D detectors irradiated at SLHC fluences and testbeam operation results; these proceedings
[21] I. Peric, The first beam test of a monolithic particle pixel detector in high-voltage CMOS technology, these proceedings
[22] W. Dulinski et al., Thin, Fully Depleted Monolithic Active Pixel Sensor with Binary Readout based on 3D Integration of Heterogeneous CMOS Layers, IEEE Nuclear Science Symposium, Orlando (25-31 October).
[23] Carlos Mariñas, The Belle-II Pixel Vertex Tracker at the SuperKEKB Flavor Factory & S. Furletov, A system for characterisation of DEPFET silicon pixel matrices and test beam results; these proceedings
[24] D. Cussans et al., Results from the ISIS1 detector; NIMA Volume 604, Issues 1-2 (2009), Pages 393-396; doi:10.1016/j.nima.2009.01.173
[25] Y. Arai, Development of SOI Pixel Detectors & L. Soung Zee, TRAPPISTe-1 Monolithic Pixel Detector in SOI Technology, these proceedings